30th NENE 2021
September 6 - 9
BLED-SLOVENIA
International Conference Nuclear Energy for New Europe

Microstructure Characterisation Of $(U,Pu)O_{2-x}$ Fuel By Raman Spectroscopy

Laetitia Medyk
DES/ISEC/DMRC/SASP/LMAT
CEA Marcoule
30200, Bagnols sur Cèze, France
mdk.laetitia@gmail.com

ABSTRACT

The uranium-plutonium mixed oxides $(U,Pu)O_{2-x}$ are currently studied as candidates for fuel of 4th generation nuclear reactors, the Sodium cooled Fast Reactors (SFR). Compared to MOX fuels used in Pressurized Water Reactors (PWR) or Evolutionary Power Reactors (EPR), these materials will contain more plutonium and have to be oxygen hypostoichiometric. The impact of these specifications on the microstructure has to be studied. Raman spectroscopy, sensitive to the local symmetry, seems to be a promising characterization tool for $(U,Pu)O_{2-x}$ material. Moreover, when the Raman spectrometer is coupled with a microscope, the properties can be determined at the micrometric scale and variation maps can be obtained. In this work, $(U,Pu)O_{2-x}$ pellets with different plutonium contents were first studied at the macroscopic scale by Raman spectroscopy, X-Ray Diffraction, Electron Probe Micro-Analysis and X-ray Absorption Spectroscopy. These characterizations demonstrated that Raman spectroscopy can be used to determine the plutonium content, the O/M ratio and identify the structural defects. Then, the Raman cartography tool was used in order to image the variation of these properties at the micrometric scale. Thereby, the heterogeneity of the cationic distribution in the pellets was mapped and the oxygen stoichiometry was quantified.

The ability of Raman microscopy for characterizing $(U,Pu)O_{2-x}$ at the micrometric scale was then demonstrated in this work.

1 INTRODUCTION

In the frame of the development of 4th generation reactors, new $(U,Pu)O_2$ fuels containing a higher Pu content (Pu/(U+Pu) > 20% mol.) are considered. To avoid the cladding corrosion in the reactor and the fuel melting, the O/M ratio, with O and M = U+Pu the molar fractions of oxygen and cations respectively, has to range between 1.94 and 2.00. However, for Pu/(U+Pu) > 20% mol. and O/M < 1.985, the ternary phase diagram of U-Pu-O exhibits a miscibility gap domain up to 800°C [1]. Thus, the material is biphasic and composed of two face-centered cubic (f.c.c.) phases, with similar Pu contents but two different O/M ratios: a rich-oxygen phase and a poor-oxygen phase. The variation of the oxygen stoichiometry between the two phases induces a lattice parameter change. The demixtion, while the material enters the miscibility gap domain, triggers crack formation, leading to the unsuitability of the fuel for its use in a reactor.

The determination of the oxygen stoichiometry and its study as a function of the Pu content is then paramount. Up to now, the techniques used to determine the O/M ratio were ThermoGravimetry Analysis (TGA), X-Ray Diffraction (XRD) or X-Ray absorption Spectroscopy (XAS). However, structural and chemical information is obtained only at the

macroscopic scale, *i.e.* the global scale, or extended to the whole sample. No technique was available to determine and map the O/M ratio at the micrometric scale, *i.e.* the local scale.
Previous to my work, several authors evidenced the potentiality of Raman spectroscopy to determine the Pu content in $(U,Pu)O_2$ samples and to detect the presence of structural defects [2]–[4]. As the variation of the oxygen stoichiometry leads to defect creation, such as oxygen vacancies, interstitial atoms, etc, the O/M ratio could be analysed by Raman spectroscopy. Moreover, coupled with an optical microscope, information can be obtained and used for mapping several properties at the micrometric scale.
The aim of my Ph. D. thesis was then to develop a Raman microscopy methodology to characterize $(U,Pu)O_{2-x}$ samples at the micrometric scale.
The first step was to decorrelate the effects of Pu content, self-irradiation and O/M ratio variations on the Raman spectra. For this purpose, XRD and Raman spectroscopy were used to analyse pellet fragments at the global scale.
The second step was to identify the defect nature associated to newly appeared Raman bands. This study was performed using XAS and Raman spectroscopy.
Finally, $(U,Pu)O_{2-x}$ pellets were analyzed at the local scale. Coupling the Raman maps with EPMA results, the O/M ratio was mapped for the first time at the micrometric scale.

2 DECORRELATION OF PU/(U+PU) CONTENT, SELF-IRRADIATION AND O/M RATIO EFFECTS

Raman microscopy is based on the interaction of a monochromatic light with the matter and allows access to the bond vibration. In a solid, the Raman active modes are determined by the symmetry. $(U,Pu)O_{2-x}$ crystallizes in a Fm-3m structure, characterized by only one first-order active mode, the T_{2g}. It corresponds to the anti-symmetrical stretching of O-M bonds. In addition, in this material, Raman spectroscopy only probes the anionic sub-lattice.

In previous studies [5], [6] it was highlighted that a variation of the lattice parameter can induce a T_{2g} shift. In $(U,Pu)O_{2-x}$ materials, self-irradiation, Pu content and O/M ratio variations lead to a lattice parameter change. This study aims to dissociate and quantify the effects of these parameters on the T_{2g} position. For this purpose, aged samples with different Pu contents (from 19 to 46 mol.%) were analysed before and after annealing. A thermal treatment was performed at 1873K to remove the defect induced by self-irradiation [7] and fix the O/M ratio to 2.00. The annealed samples were then considered as without defect.

2.1 Lattice parameter and O/M ratio determination by XRD analysis

XRD analysis allowed determining the lattice parameter of aged and annealed samples. From this value, O/M ratio can be calculated *via* Duriez's law [8]:

$$a = 5.45 - 0.074y + 0.32x \quad \text{Eq. (1)}$$

(with y the Pu molar fraction and x the deviation from stoichiometry).
Self-irradiation induces a swelling and the O/M ratio has to be calculated from a corrected lattice parameter. The increase is quantified thanks to a relation given by Kato *et al.* [9].

All the annealed samples were stoichiometric, which allowed a comparison with the literature [2], [3], [6], [10]. Half of the aged samples was stoichiometric and the other part was hypostoichiometric.

2.2 Raman spectroscopy

For all the samples, a minimum of three spectra was recorded to obtain an average spectrum and avoid the effect of a potential heterogeneity. The T_{2g} band position for each sample was obtained from these average spectra. The Figure 1a) represents the T_{2g} position as a function of the lattice parameter of annealed and stoichiometric samples (green triangles). Results from literature were plotted to compare and to extend the lattice parameter range.
In Figure 1b), aged samples are represented in addition of the annealed samples of this work. Two types of lattice parameters are attributed to the aged samples: the raw one, directly obtained from the XRD pattern (red squares), and the one corrected from self-irradiation contribution (blue points).

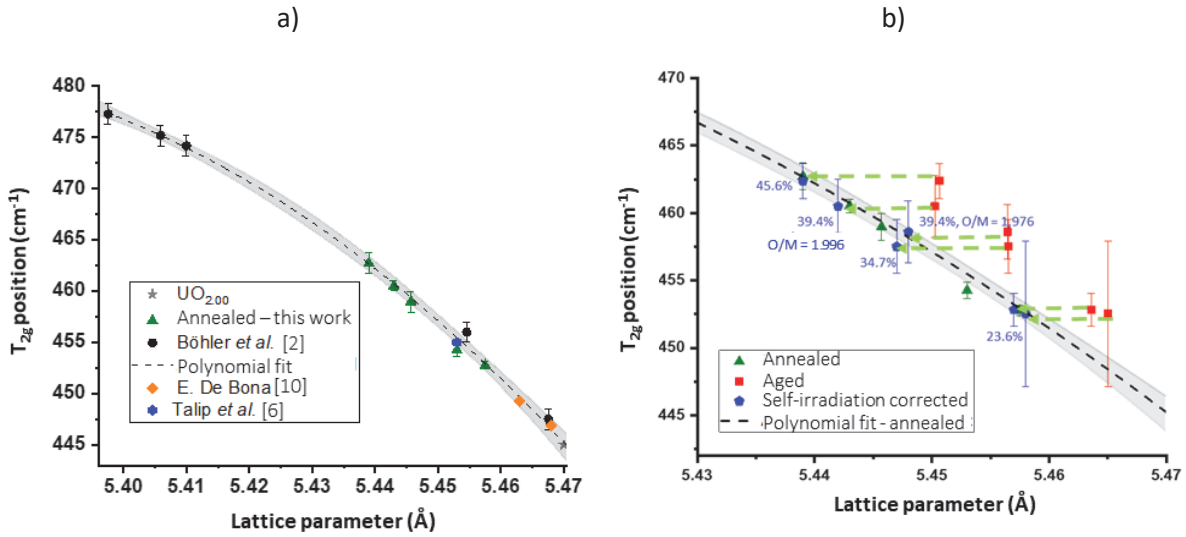

Figure 1: T_{2g} position as a function of lattice parameter a) for annealed samples of this work (green triangles) and literature data [2], [6], [10], b) for aged samples with the raw lattice parameter (red points) and corrected from self-irradiation contribution (blue points).

In Figure 1a), a polynomial function of degree 2 can be used to fit the data of the annealed and stoichiometric samples. In this case, x, the deviation from stoichiometry is equal to 0 and the lattice parameter is directly linked to the Pu content (*c.f.* Eq. (1)). From the polynomial equation, **the lattice parameter, and therefore the Pu content, can be determined from the T_{2g} position for annealed and stoichiometric samples.**
In Figure 1b), this polynomial function is plotted as well as the annealed and stoichiometric sample points as references. The raw lattice parameters for aged samples are above this line, without any regular trend while the ones corrected from self-irradiation can be fitted using the polynomial function. **This observation highlights the fact that self-irradiation has no impact on the T_{2g} position.**
Moreover, the T_{2g} position always follows the polynomial function whether the lattice parameter variation is due O/M ratio or the Pu content.
However, by considering only the T_{2g} band position, distinguishing the contribution of these two properties is impossible. To this aim, the whole Raman spectrum will be analyzed in the next part.

3 DEFECT IDENTIFICATION

Structural or chemical defects can be found in $(U,Pu)O_2$ samples due to self-irradiation, deviation from stoichiometry or Pu content variation. Their presence leads to lattice distortion and the symmetry is locally broken. Thus, in Raman spectra, new bands appear. The effects of self-irradiation were already studied in the literature and the appearance of a band triplet, commonly named U1, U2 (or $T_{1u}LO$) and U3, was highlighted [4], [6]. The U3 band was attributed in the literature to oxygen clusters similar of the ones in U_4O_8 [11]. The U1 band seems to be correlated to hypostoichiometry defects, as already seen for $(U,Ln)O_{2-x}$ samples [12].
The exact attribution of their presence in $(U,Pu)O_{2-x}$ can be helpful to dissociate the contribution of self-irradiation, deviation from stoichiometry and Pu content variation. To this aim, X-ray Absorption Spectroscopy (XAS) measurements were performed, in addition of Raman spectroscopy, on aged and hypostoichiometric samples and annealed and stoichiometric samples. Annealed and hypostoichiometric samples were also prepared for XAS measurements, unfortunately during storage and transport, a re-oxidation occurred. They were then only analysed by Raman spectroscopy.

3.1 X-ray Absorption Spectroscopy

X-ray Absorption Spectroscopy is based on the interaction between the matter and photons. It consists in determining the absorption energies of the X-ray photons, which result from the ejection of a bound electron towards a free energy level. The absorption thresholds, corresponding to the ejection energy of the electron, can be determined for the different orbitals. The energies are function of the element and the atom oxidation state. X-ray absorption spectroscopy is therefore chemically selective.
A XAS spectrum is divided into two zones:

- the XANES (X-ray Absorption Near the Edge Structure) gives information on the electronic structure and the valence state of the atom considered as well as the local symmetry.
- the EXAFS (Extended X-Ray Absorption Fine Structure) gives information on the local environment of the atom, such as the distance, nature, disorder and number of neighbour atoms for each coordination sphere around the probed element.

In this work, XANES spectra were collected at the M_4 thresholds of U and Pu, and L_3 of Pu and Am (present due to Pu decay for more than 20 years). The spectra allowed determining the oxidation states, the ion proportion and thus, the O/M ratio. Surprisingly, even if $(U,Pu)O_{2.00}$ samples were stoichiometric, U^{5+} and Pu^{3+} were also present in the sample, in addition of U^{4+} and Pu^{4+}. Moreover, americium was only present in its trivalent state.
EXAFS spectra were measured at the U-L_3 and Pu-L_2 thresholds and allowed determining U-M, Pu-M, and M-O distances, with M = U or Pu. It was highlighted that, in every sample, Pu-O and U-O distances were always different, leading to a lattice distortion. Furthermore, no oxygen clusters were identified, although they could be in too low concentration to be detected.

3.2 Raman spectroscopy

Average Raman spectra, measured on both the annealed and hypostoichiometric samples, are represented on Figure 2.

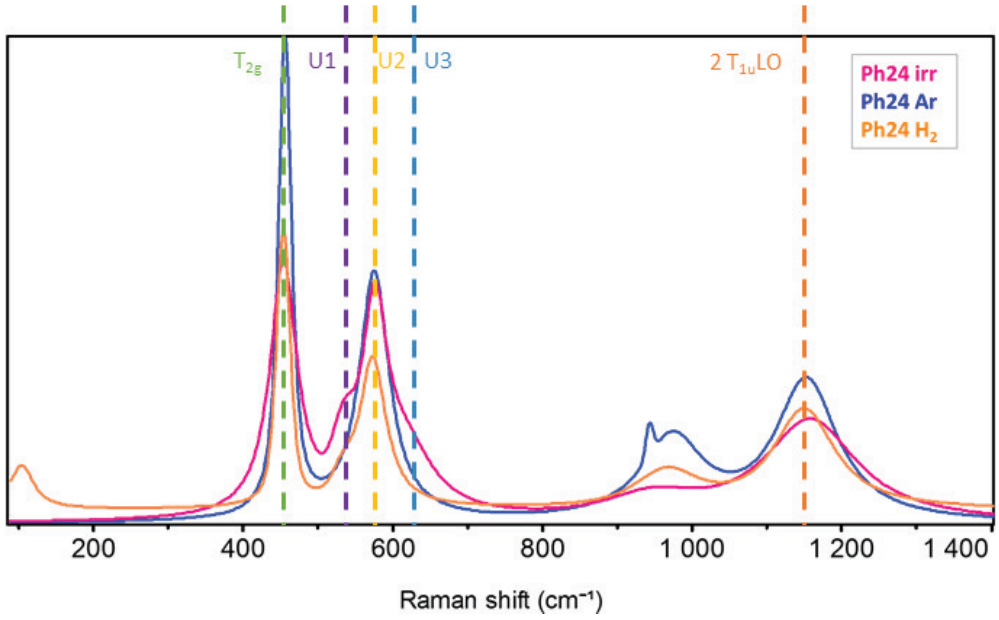

Figure 2: average of more than 3000 Raman spectra on $U_{0.76}Pu_{0.24}O_{2-x}$ samples, aged and stoichiometric (pink), annealed and stoichiometric (blue), annealed and hypostoichiometric (orange).

On each spectrum, the bands T_{2g}, $T_{1u}LO$ and 2 $T_{1u}LO$ are present but with different intensities. The spectrum of aged sample is the only one presenting the triplet of defect bands, however the U1 band is also visible on the spectrum of hypostoichiometric sample.

Coupling these observations with the results from the XAS study and the literature, the spectral variations were then attributed to defects:

- For the annealed and stoichiometric samples, a single defect band $T_{1u}LO$ is present. Its appearance is probably due to the deformation of the local symmetry generated by the difference between U-O and Pu-O distances.

- As the U3 band is present only on the spectra of the aged samples, its attribution to oxygen defect clusters remains valid.

- The U1 band seems to be associated with defects induced by hypostoichiometry and self-irradiation.

This study has therefore allowed us to dissociate the effects of self-irradiation and hypostoichiometry on the whole Raman spectrum and the different types of defects have been associated to a spectral variation. All these observations were made at the macroscopic scale. The following part will therefore focus on the characterization of these properties and their variations within a sample and at the scale of ceramic grains (µm).

4 RAMAN MAPS OF PU CONTENT AND O/M RATIO

When the Raman spectrometer is coupled to a microscope, the properties can be obtained at a scale determined by the magnification of the optical objective used. For example, using a magnification of x100, the surface of the laser spot is of the order of μm^2. Thus, the Raman mapping tool consists in selecting an area on the surface of a solid sample, dividing it by a mesh and collecting spectra at each point. Then, to perform the imaging, one characteristic of one band of the spectra is considered, for instance the T_{2g} position, and each value is associated to a colour. Thus, the variation of various microstructural properties can be mapped.

As previously described in section 2, the T_{2g} position is linked to the lattice parameter, and, for stoichiometric samples, to the Pu content. To verify these results and the mapping processing, a $(U,Pu)O_{2.00}$ sample was analysed at the same area by Raman microscopy and Electron Probe Micro-Analysis (EPMA). This technique is dedicated to surface analyses by Wavelength Dispersive Spectroscopy (WDS) giving access to the chemical composition of samples. It is based on the interaction between an electron beam and the material. The electrons excite the atoms constituting the matter. When they return to their fundamental state, they emit X-ray photons whose energy is specific to each element. The number of X-rays emitted with the same energy is function of the element concentration. With the use of standards and the correction of matrix effect, this technique allows the quantification of each element.

A comparison between EPMA and T_{2g} position Raman maps, converted into Pu content, is represented in Figure 3.

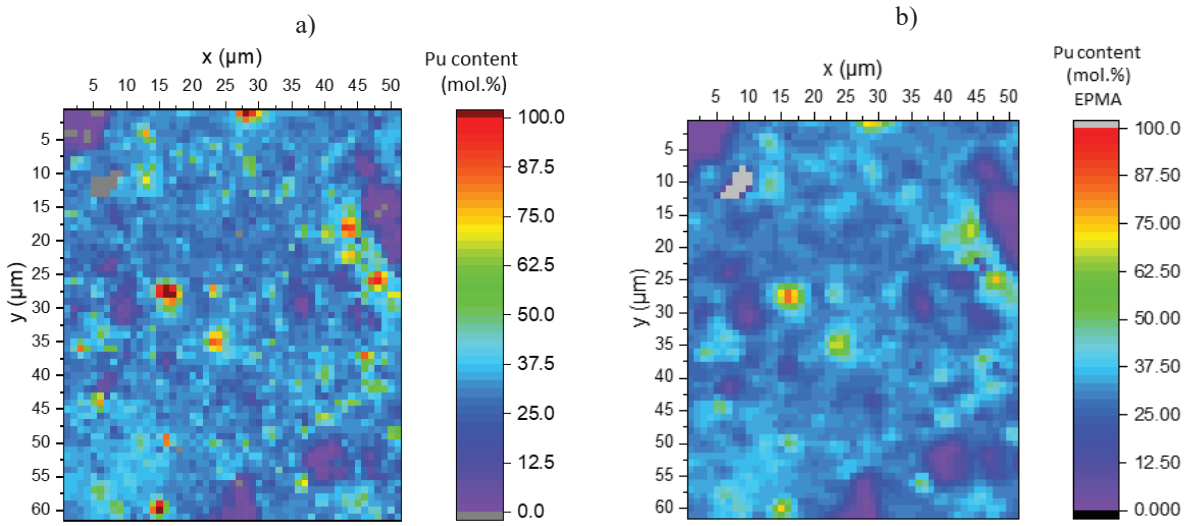

Figure 3: Pu content (%.mol) obtained by Raman microscopy from the T_{2g} position and by EPMA. Grey points are porosities.

The two maps were found in very good agreement, exhibiting similar Pu contents. Then, the mapping processing allows the coupling of EPMA and Raman maps to determine the Pu content and properties associated to Raman feature at each pixel. Using this methodology, the lattice parameter and the Pu content were first obtained at each (x,y) point with Raman and EPMA maps respectively. The O/M ratio was then determined according to Eq. (1) at each pixel. The resulting map, obtained on an hypostoichiometric $(U,Pu)O_{2-x}$ sample, is shown in Figure 4.

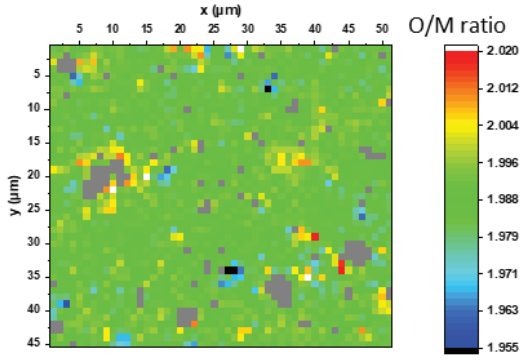

Figure 4: O/M ratio cartography determined from Raman and EPMA maps performed on the same area. Grey points correspond to deleted spectra due to a lack of Raman signal.

Different information was obtained from this acquisition such as the graph in Figure 5a) representing the O/M ratio as a function of Pu content. As previously explained, specific combinations of these two parameters can lead to the entrance of the material in a miscibility gap domain, resulting in a demixtion in two phases. The points gathering the conditions for its appearance are located in the orange rectangle (O/M < 1.985 and y > 0.2) and highlighted as dashed blue/white in the Figure 5b).

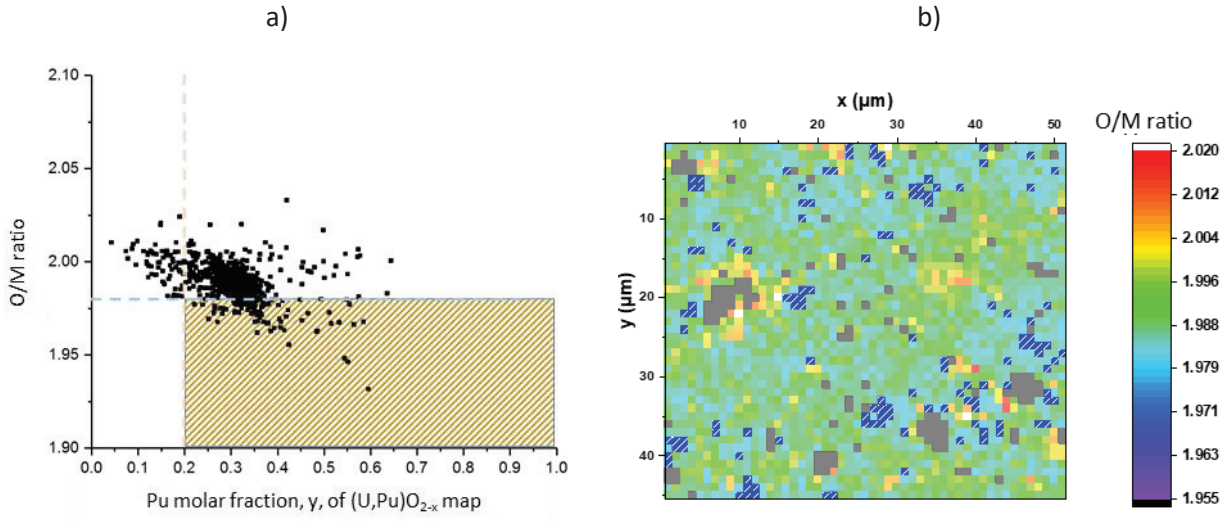

Figure 5: a) O/M ratio as a function of y, the molar fraction of Pu in $(U,Pu)O_{2-x}$, in the analyzed zone. The hatched rectangle corresponds to the miscibility gap domain. b) O/M ratio cartography. The points corresponding to the miscibility gap domain are in blue with white stripes.

Although the O/M ratio obtained from XRD analyses was higher than 1.985, meaning that the material was not in the miscibility gap domain, the Raman analysis at a lower scale demonstrated that, due to heterogeneities in the Pu content distribution, some spots gathered these conditions.

These results were obtained initially from the T_{2g} position map, but, as explained here, other information was determined from other band feature such as defect presence and nature by considering U1 or U3 intensity bands. By collecting several Raman maps, correlations were deduced between the different properties and a full characterization was performed.

5 CONCLUSION AND PERSPECTIVES

My Ph.D. work aimed at developing a Raman microscopy technique for the characterization of the Pu content, the O/M ratio and the detection of structural defects in $(U,Pu)O_{2-x}$ pellets.

First, a macroscopic study was performed by Raman spectroscopy, XRD and XAS. It was demonstrated that several properties affect the Raman spectra and their variation were attributed to spectrum features. Thus, the determination of the lattice parameter *via* the T_{2g} position was made possible, self-irradiation defects were detected based on the presence of a triplet band and hypostoichiometry leaded to the appearance of the U1 band.

The second part of the work was the microscopic study and sample characterization *via* Raman maps. Based on the previous results, the Pu content map was obtained with the same resolution as an EPMA map. Coupling the latter with Raman map on the same area, O/M ratio map was obtained for the first time, highlighting that the miscibility gap can be present even if the global O/M ratio indicates a monophasic material.

This thesis work has thus demonstrated the interest of Raman microscopy for the microstructure characterization of (U,Pu)O_2 fuels at the micrometric scale. This opens the way to numerous complementary studies. For example, a consideration of other bands would be a possibility to quantify the Pu content and thus use the position of the T_{2g} band to determine the O/M ratio. Raman microscopy could then be used without the combination of other methods to map the oxygen stoichiometry and be implemented as a control tool in an industrial scale production line.

Finally, thanks to a heating cell dedicated to *in situ* Raman measurements, many applications can be envisaged. By controlling the oxygen partial pressure, phase transitions of the U-Pu-O system can be observed, extending the knowledge of the phase diagram based on the anionic sub-lattice. By heating at high temperature, the annealing of defects can be studied and would allow validating the attribution of their bands. In these two applications, kinetic studies, rare on this type of material, can also be conducted.

REFERENCES

[1] C. Guéneau *et al.*, « Thermodynamic modelling of advanced oxide and carbide nuclear fuels: Description of the U–Pu–O–C systems », *J. Nucl. Mater.*, vol. 419, nº 1–3, Art. nº 1–3, déc. 2011, doi: 10.1016/j.jnucmat.2011.07.033.

[2] R. Böhler *et al.*, « Recent advances in the study of the UO_2–PuO_2 phase diagram at high temperatures », *J. Nucl. Mater.*, vol. 448, nº 1–3, Art. nº 1–3, mai 2014, doi: 10.1016/j.jnucmat.2014.02.029.

[3] J. M. Elorrieta *et al.*, « Raman study of the oxidation in (U, Pu)O_2 as a function of Pu content », *J. Nucl. Mater.*, vol. 495, nº Supplement C, Art. nº Supplement C, nov. 2017, doi: 10.1016/j.jnucmat.2017.08.043.

[4] C. Jegou *et al.*, « Raman micro-spectroscopy of UOX and MOX spent nuclear fuel characterization and oxidation resistance of the high burn-up structure », *J. Nucl. Mater.*, vol. 458, p. 343-349, mars 2015, doi: 10.1016/j.jnucmat.2014.12.072.

[5] H. Li, P. Zhang, G. Li, J. Lu, Q. Wu, et Y. Gu, « Stress measurement for nonstoichiometric ceria films based on Raman spectroscopy », *J. Alloys Compd.*, vol. 682, p. 132-137, oct. 2016, doi: 10.1016/j.jallcom.2016.04.272.

[6] Z. Talip *et al.*, « Raman microspectroscopic studies of unirradiated homogeneous ($U_{0.76}Pu_{0.24}$)O_{2+x}: the effects of Pu content, non-stoichiometry, self-radiation damage and secondary phases », *J. Raman Spectrosc.*, p. n/a-n/a, janv. 2017, doi: 10.1002/jrs.5092.

[7] D. Staicu, T. Wiss, V. V. Rondinella, J. P. Hiernaut, R. J. M. Konings, et C. Ronchi, « Impact of auto-irradiation on the thermophysical properties of oxide nuclear reactor fuels », *J. Nucl. Mater.*, vol. 397, nº 1, Art. nº 1, févr. 2010, doi: 10.1016/j.jnucmat.2009.11.024.

[8] C. Duriez, J.-P. Alessandri, T. Gervais, et Y. Philipponneau, « Thermal conductivity of hypostoichiometric low Pu content (U,Pu)O_{2-x} mixed oxide », *J. Nucl. Mater.*, vol. 277, nº 2–3, Art. nº 2–3, févr. 2000, doi: 10.1016/S0022-3115(99)00205-6.

[9] M. Kato *et al.*, « Self-radiation damage in plutonium and uranium mixed dioxide », *J. Nucl. Mater.*, vol. 393, nº 1, Art. nº 1, août 2009, doi: 10.1016/j.jnucmat.2009.05.020.

[10] E. de Bona, « Grain size effects on radiogenic Helium gas in the nuclear fuel UO_2 », phdthesis, Université Paris-Saclay, 2019. https://tel.archives-ouvertes.fr/tel-02640436

[11] L. Desgranges, G. Baldinozzi, P. Simon, G. Guimbretière, et A. Canizares, « Raman spectrum of U_4O_9: a new interpretation of damage lines in UO_2 », *J. Raman Spectrosc.*, vol. 43, nº 3, Art. nº 3, mars 2012, doi: 10.1002/jrs.3054.

[12] Z. Talip *et al.*, « Raman and X-ray Studies of Uranium–Lanthanum-Mixed Oxides Before and After Air Oxidation », *J. Am. Ceram. Soc.*, vol. 98, nº 7, Art. nº 7, juill. 2015, doi: 10.1111/jace.13559.